

## Review

# Hydrogen production through sorption-enhanced steam methane reforming and membrane technology: A review

L. Barelli\*, G. Bidini, F. Gallorini, S. Servili

*Department of Industrial Engineering, University of Perugia, Via G. Duranti 1/A4, Perugia 06125, Italy*

Received 16 May 2007

**Abstract**

With the rapid development of industry, more and more waste gases are emitted into the atmosphere. In terms of total air emissions, CO<sub>2</sub> is emitted in the greatest amount, accounting for 99 wt% of the total air emissions, therefore contributing to global warming, the so-called “Greenhouse Effect”. The recovery and disposal of CO<sub>2</sub> from flue gas is currently the object of great international interest. Most of the CO<sub>2</sub> comes from the combustion of fossil fuels in power generation, industrial boilers, residential and commercial heating, and transportation sectors. Consequently, in the last years’ interest in hydrogen as an energy carrier has significantly increased both for vehicle fuelling and stationary energy production from fuel cells. The benefits of a hydrogen energy policy are the reduction of the greenhouse effect, principally due to the centralization of the emission sources. Moreover, an improvement to the environmental benefits can be achieved if hydrogen is produced from renewable sources, as biomass.

The present paper provides an overview of the *steam methane reforming* (SMR) process and methodologies for performances improvement such as hydrogen removal, by selective permeation through a membrane or simultaneous reaction of the targeted molecule with a chemical acceptor, and equilibrium shift by the addition of a CO<sub>2</sub> acceptor to the reactor.

In particular, attention was focused on the *sorption-enhanced steam methane reforming* (SE-SMR) process in which sorbents are added in order to enhance the reactions and realize in situ CO<sub>2</sub> separation. The major operating parameters of SE-SMR are described by the authors in order to project and then realize the innovative carbonation reactor developed in previous studies.

© 2007 Elsevier Ltd. All rights reserved.

**Keywords:** Hydrogen; SMR; CO<sub>2</sub> capture; Solid acceptor; SE-SMR

**Contents**

1. Introduction . . . . .	555
2. Hydrogen production through traditional steam methane reforming (SMR) process . . . . .	556
2.1. The SMR process . . . . .	556
2.2. PSA process . . . . .	557
2.3. Kinetic model of SMR process . . . . .	557
3. Improving hydrogen production . . . . .	558
3.1. Membranes . . . . .	559
3.1.1. OTM + HTM membrane with porous ceramic substrate and palladium film coating . . . . .	559
3.1.2. Ion transport membrane (ITM) . . . . .	560
3.2. Sorption enhanced SMR using CO <sub>2</sub> sorbent . . . . .	561
3.2.1. Kinetic models and parameters for SE-SMR . . . . .	563

\*Corresponding author. Tel.: +39 075 5853740; fax: +39 075 5853736.

E-mail address: [barelli@unipg.it](mailto:barelli@unipg.it) (L. Barelli).

3.2.2.	Temperature and pressure influence on SE-SMR and performances comparison with SMR. . . . .	565
3.2.3.	Experimental activities about the characterization of some SE-SMR performances. . . . .	567
4.	Conclusions . . . . .	568
	References . . . . .	569

## 1. Introduction

There are different hydrogen production processes that can each be used for several of the feedstock options. Hydrogen can be produced in large central facilities, as *integrated gasification combined cycle (IGCC)* coal plant (that could provide power, hydrogen, liquid fuels, and chemicals all at one site), or *biorefinery* using a biomass feedstock gasification process, and then distributed to the area of use.

Moreover, it can be produced also in a semi-distributed fashion near larger market centres such as urban centres and urban corridors, or directly to the area of use such as existing transportation refuelling stations or even in a home or commercial building. Finally, it can be produced from hydrogen-rich liquid fuels in onboard reformers.

As concerns the central or semi-distributed cases, hydrogen can be delivered through a variety of means including new dedicated hydrogen pipelines, liquid transport via truck or rail, or possibly using new solid hydrides as a result of successful research.

Some options are better suited for central production, while others are better suited for semi-distributed and local production. The cost and energy needed to distribute and deliver hydrogen is a major contributing factor because of its relatively low energy density. Further research and development will be needed to achieve competitive costs for hydrogen compared with conventional energy systems in use in the marketplace today; however, some options are closing in on cost goals.

Relatively to the feedstock supply, fossil fuels are an obvious choice as energy resources for the production of the large quantities of hydrogen needed to begin the transition to a sustainable hydrogen economy. Infact, in the transition phase, the need of considerable cost reduction and technical improvements throughout the entire hydrogen system (production, delivery, storage, conversion, and application) arises. To this aim, attention is currently focused on natural gas and coal.

Hydrogen, infact, for industrial and commercial use is produced from steam reforming of natural gas, as discussed later, with attendant water–gas shift (WGS) reactions. This is a mature technology widely used in the petroleum processing industry. Significant opportunities exist for the development of new technologies with the potential to reduce the costs of hydrogen production from natural gas. Another fossil fuel–coal can also be an energy source for producing hydrogen. With associated carbon dioxide capture and sequestration technologies, hydrogen from natural gas and coal can make significant contributions toward achieving “zero emission” power plants.

Therefore, today, there is significant hydrogen production from coal gasification and the subsequent processing of the synthesis gas. Moreover, coal-derived synthesis gas can be converted to methanol for use both as an intermediate product in the chemical industry and a hydrogen carrier for subsequent reforming applications.

Coal gasification is a promising technology for the combined production of electric power, based on IGCC technology, and hydrogen. On February 27, 2003, USA Secretary of Energy announced the FutureGen initiative to design, build, and operate the world’s first coal-fired, zero emissions plant integrated with carbon sequestration. The goal of the project is to produce electricity at a cost increase no greater than 10% relative to non-sequestered systems, and hydrogen at a cost of \$4.00/MMBtu. In such a plant, gasification combines coal, oxygen and steam to produce synthesis gas that is cleaned of impurities such as sulphur or mercury. To produce hydrogen, such synthesis gas is shifted using mature WGS reactor technology to generate additional hydrogen and convert carbon monoxide to carbon dioxide. Hydrogen is subsequently separated from the gas stream. Currently, this separation is accomplished through the use of mature *pressure swing adsorption (PSA)* technology which operates near its theoretical limit. The residual gas from this separation can be recycled or combusted. The synthesis gas can also be converted into hydrocarbons and oxygenates for upgrading to liquid transportation fuels, or reformable fuels to produce hydrogen for fuel cell applications.

Carbon dioxide produced in the hydrogen production process is removed utilizing capture and sequestration technology. In order to reduce costs, novel and advanced technology must be developed in all phases of the gasification/hydrogen production and separation process, now being developed in an associated program.

In particular within the Hydrogen from Coal Program, R&D activities are focused on the development of novel processes that include:

- advanced WGS reactors using sulphur-tolerant catalysts to produce more hydrogen from synthesis gas at lower cost;
- novel membranes for advanced and lower cost hydrogen separation from carbon dioxide and other contaminants;
- advanced technology concepts that combine hydrogen separation and the WGS reaction;
- technologies that utilize fewer steps to separate carbon dioxide, hydrogen sulphide, and other impurities from hydrogen.

## Nomenclature

SMR	steam methane reforming
SE-SMR	sorption-enhanced steam methane reforming
PSA	pressure swing adsorption
SERP	sorption enhanced reaction process
WGS	water gas shift reaction
OTM	oxygen transport membranes
HTM	hydrogen transport membranes
ITM	ion transport membranes
IMTL	inorganic membranes developed by inorganic membrane technology laboratory
PM <sub>10</sub>	particulate matter with diameter less 10 μm
$\Delta H_{298}^0$	heat of reaction (kJ/kmol)
$R$	reaction rates
$P$	pressure
$k$	Reaction rate constant

$K_{eq}$	equilibrium constants
$K$	species adsorption constants
$r$	formation or consumption rate
$S/C$	steam to carbon ratio
$T$	time required to completely convert an un-reacted particle into product in equation
$X$	fractional mass conversion
$\Psi$	structural parameter depending on the surface area, porosity, and the initial total length of pore system per unit volume
$Y$	gas-phase mole fraction

## Subscripts

$j$	equation number, referring to steam methane reforming reactions
$i$	species CH <sub>4</sub> , H <sub>2</sub> O, H <sub>2</sub> , CO, CO <sub>2</sub>

At the same time, cost reduction and process efficiency improvements are dependent upon R&D successes, relative to coal gasification technologies, which include:

- advanced *ion transport membranes* (ITM) technology for oxygen separation from air;
- advanced cleaning of raw synthesis gas;
- improvements in gasifier design, materials and feed systems;
- carbon dioxide capture and sequestration technology.

In relation to all these R&D successes, carbon dioxide emissions could be strongly reduced eliminating public concerns over the generation of greenhouse gas emission. Criteria pollutants of SO<sub>x</sub>, NO<sub>x</sub>, and PM<sub>10</sub> could be also significantly reduced. Moreover, production of low-cost hydrogen from coal could reduce reliance on imported oil. In such way, hydrogen from coal provides a mid-term transitional source of energy until the long-term goal, of producing hydrogen significantly from renewable (biomass gasification) energy, is realized.

## 2. Hydrogen production through traditional steam methane reforming (SMR) process

### 2.1. The SMR process

The dominant industrial process used to produce hydrogen is the SMR process [1]; it has been in use for several decades as an effective mean for hydrogen production. SMR of natural gas is a mature technology, operating at or near the theoretical limits of the process that is used to produce nearly all the hydrogen (in the form of a mixture of hydrogen and carbon monoxide) in the chemical industry and the supplemental hydrogen in refineries.

A process for the conversion of hydrocarbons into hydrogen in the presence of steam was first described by

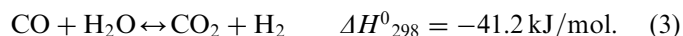
Tessie du Motay and Marechal in 1868 [2]. The first industrial application of SMR was implemented in 1930. The feedstock for this process includes methane, naphtha and no 2 fuel oil.

The SMR process is characterized by multiple-step and harsh reaction conditions [3]. SMR is a catalytic process that involves a reaction between natural gas or other light hydrocarbons and steam. The result is a mixture of hydrogen, carbon monoxide, carbon dioxide and water that is produced in a series of three reactions. Relative to the schematic flowsheet for a conventional SMR process shown in Fig. 1, the first reforming step (Eqs. (1) and (2)) catalytically reacts methane with steam fed into the reformer furnace, to form hydrogen and carbon monoxide in an endothermic reaction.



These reactions are typically carried out at a temperature of 800–1000 °C and a pressure of 14–20 atm over a nickel-based catalyst. The reforming reaction is highly endothermic and a large amount of heat is provided by feeding supplemental natural gas to the furnace. The effluent gas from the reformer contains about 76% H<sub>2</sub> (mol%), 13% CH<sub>4</sub>, 12% CO and 10% CO<sub>2</sub> on a dry basis [4].

Then the reformer products are fed to a WGS reactor where the following reaction (Eq. (3)) occurs:



Reaction expressed by Eq. (3) is moderately exothermic and is therefore favoured by low temperatures.

Therefore, when considering the operative high temperature above 750 °C needed for a substantial reforming conversion of CH<sub>4</sub>, the produced gas is characterized by a 8–10% CO content on a dry basis [5]. To reduce CO content at the outlet of the SMR reactor, the syngas

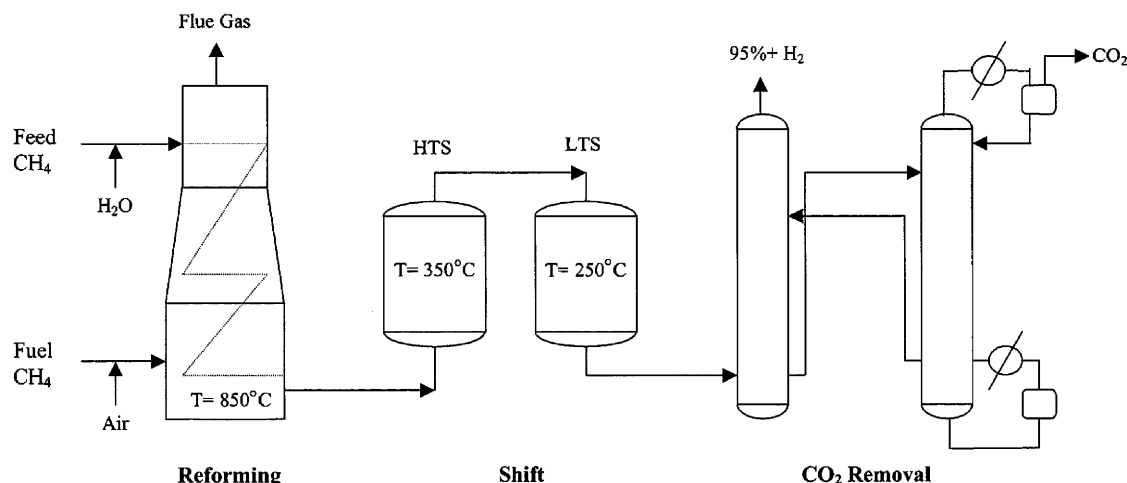


Fig. 1. Flowsheet for a conventional SMR process.

produced is conventionally fed to WGS reactor where the temperature is kept as low as 300–400 °C to favour the WGS reaction. Downstream, when high purity H<sub>2</sub> is desired (up to 99%), normally either PSA technology or amine scrubbing is used to remove CO<sub>2</sub>.

Moreover, when hydrogen is used in downstream catalytic processes (fuel cells), the final CO concentration is well above the allowable levels due to the equilibrium limited of the exothermic shift reaction. In such cases methanation and preferential oxidation (PROX) can be used to remove CO.

## 2.2. PSA process

The current technology used to separate hydrogen from synthesis gas is PSA, widely applied in gas purification and recovery. Main fields of application are in fact the recovery and purification of hydrogen, carbon dioxide removal and purification, methane purification as well as nitrogen and oxygen generation.

The essentials of PSA are [6]:

1. improved and established technology, even if the process is comparably young (industrial application started in the 1970s);
2. reliability with availabilities higher than 99%;
3. flexibility (typical operation range is 25–100%);
4. fully automated operation even at pressure, temperature and flow fluctuation.

Higher product purities are achievable with high recovery rates up to 99% and more. Hydrogen recovery PSA units are usually integrated in larger grids, for example hydrogen recovery units processing a shifted raw hydrogen gas from a steam reformer. The tail gas is recycled to the reformer burners, the hydrogen product is fed into the plant's hydrogen grid. Therefore, the attractiveness of the PSA

methods stems from the fact that even complex separations can be regarded as a sequence of several relatively simple steps.

The cycle can be divided into phases whose number equals the number of columns in the unit. The basic steps, included in the majority of modern PSA cycles, are [7]:

1. adsorption, at a constant pressure  $p_H$ ;
2. regeneration (purge), at a constant pressure  $p_{purge}$ ;
3. pressure equalization:
  - cocurrent/countercurrent;
  - countercurrent/cocurrent;

the first term refers to the direction of flow in the column undergoing depressurization (pressure  $p$  decreases from  $p \leq p_H$  to  $p > p_{purge}$ ), whereas the second term describes the direction of flow in the column being pressurized ( $p$  increases from  $p \geq p_{purge}$  up to  $p < p_H$ );
4. depressurization:
  - cocurrent ( $p$  changes from  $p \leq p_H$  to  $p > p_{purge}$ );
  - countercurrent ( $p$  changes from  $p \leq p_H$  to  $p \geq p_{purge}$ );
5. pressurization:
  - with the feed gas, cocurrent;
  - with the product, countercurrent.

The pressure in both of the above steps may change from  $p \geq p_{purge}$  to  $p \leq p_H$ .

## 2.3. Kinetic model of SMR process

About the kinetic model of SMR, several rate models [8–10] have been analysed in the study; anyway the authors have decided to focus the attention on the model proposed by Xu and Froment [11] because the most general and extensively tested. According to such models, the reaction kinetic of the traditional SMR using a nickel-based

Table 1  
Kinetic parameters for SMR kinetic over Ni-based catalyst

Pre-factor	Value	Unit	Energy	Value	Unit
(1) Reaction rate constants: $k_j = k_{0j} \exp(-E_j/R_g T)$ ( $j = 1, 2, 3$ )					
$k_{0,1}$	$4.225 \times 10^{15}$	kmol bar <sup>0.5</sup> /kg-cat h	$E_1$	240.1	kJ/mol
$k_{0,2}$	$1.955 \times 10^6$	kmol bar/kg-cat h	$E_2$	67.13	kJ/mol
$k_{0,3}$	$1.020 \times 10^{15}$	kmol bar <sup>0.5</sup> /kg-cat h	$E_3$	243.9	kJ/mol
(2) Species adsorption constants: $K_i' = K_{0i} \exp(-\Delta H_i/R_g T)$ ( $i = \text{CO}, \text{H}_2, \text{CH}_4, \text{H}_2\text{O}$ )					
$K_{0,\text{CO}}$	$8.230 \times 10^{-5}$	bar <sup>-1</sup>	$\Delta H_{\text{CO}}$		kJ/mol
$K_{0,\text{H}_2}$	$6.120 \times 10^{-9}$	bar <sup>-1</sup>	$\Delta H_{\text{H}_2}$		kJ/mol
$K_{0,\text{CH}_4}$	$6.640 \times 10^{-4}$	bar <sup>-1</sup>	$\Delta H_{\text{CH}_4}$		kJ/mol
$K_{0,\text{H}_2\text{O}}$	$1.770 \times 10^{-5}$	(dimensionless)	$\Delta H_{\text{H}_2\text{O}}$		kJ/mol
(3) Equilibrium constants					
$K_{\text{eq},1}$	$\exp(-26830/T + 30.114)$	bar <sup>2</sup>			
$K_{\text{eq},2}$	$\exp(4400/T - 4.036)$	(dimensionless)			
$K_{\text{eq},3}$	$K_{\text{eq},1} K_{\text{eq},2}$				

catalyst, can be summarized as

$$R_1 = \left( \frac{k_1}{P_{\text{H}_2}^{2.5}} \right) \frac{\left( P_{\text{CH}_4} P_{\text{H}_2} - \frac{P_{\text{CO}} P_{\text{H}_2}^3}{K_{\text{eq}1}} \right)}{DEN^2}, \quad (4)$$

$$R_2 = \left( \frac{k_2}{P_{\text{H}_2}^{3.5}} \right) \frac{\left( P_{\text{CH}_4} P_{\text{H}_2\text{O}}^2 - \frac{P_{\text{CO}_2} P_{\text{H}_2}^4}{K_{\text{eq}2}} \right)}{DEN^2}, \quad (5)$$

$$R_3 = \left( \frac{k_3}{P_{\text{H}_2}} \right) \frac{\left( P_{\text{CO}} P_{\text{H}_2\text{O}} - \frac{P_{\text{CO}_2} P_{\text{H}_2}}{K_{\text{eq}3}} \right)}{DEN^2}, \quad (6)$$

$$DEN = 1 + K_{\text{CO}} P_{\text{CO}} + K_{\text{H}_2} P_{\text{H}_2} + K_{\text{CH}_4} P_{\text{CH}_4} + K_{\text{H}_2\text{O}} \left( \frac{P_{\text{H}_2\text{O}}}{P_{\text{H}_2}} \right), \quad (7)$$

where

- $R_j$  ( $j = 1, 2, 3$ ) are the reaction rates of the reaction 1, 2, 3, respectively;
- $P_i = y_i P$  ( $i = \text{CH}_4, \text{H}_2\text{O}, \text{H}_2, \text{CO}, \text{CO}_2$ ) are the partial pressures of any species  $i$ , with  $y_i$  the gas-phase mole fraction of component  $i$  and  $P$  the local total pressure;
- $k_j$  are the reaction rate constant defined by Arrhenius  $k_j = k_{0j} \exp(-E_j/RT)$ ;
- $K_{\text{eq},j}$  ( $j = 1, 2, 3$ ) are the equilibrium constants;
- $K_i$  ( $i = \text{CH}_4, \text{H}_2\text{O}, \text{H}_2, \text{CO}, \text{CO}_2$ ) are the species adsorption constants of any species  $i$  defined as  $K_i = K_{0i} \exp(-\Delta H_i/RT)$ .

For the expression of the constants, see Table 1 [11].

The formation or consumption rate of component  $i$ ,  $r_i$ , was then calculated by using Eqs. (4)–(6) as follows:

$$r_i = \sum v_{ij} R_j \quad (i = 1-5), \quad (8)$$

where  $v_{ij}$  is the stoichiometric coefficient of component  $i$ . Referring to a reactant,  $v_{ij}$  is negative, while for a product,  $v_{ij}$  is positive. Thus results:

$$r_{\text{CH}_4} = -(R_1 + R_2), \quad (9)$$

$$r_{\text{H}_2\text{O}} = -(R_1 + 2R_2 + R_3), \quad (10)$$

$$r_{\text{H}_2} = 3R_1 + 4R_2 + R_3, \quad (11)$$

$$r_{\text{CO}} = R_1 - R_3, \quad (12)$$

$$r_{\text{CO}_2} = R_2 + R_3. \quad (13)$$

### 3. Improving hydrogen production

Although the SMR process has been used for many years, there is room for improvement. This process is highly energy intensive and expensive alloy reformer tubes must be used to withstand the severe operating conditions. In particular, SMR is normally carried out at 800–900 °C and 15–30 × 10<sup>5</sup> Pa, with nickel on an alumina support as the catalyst. A typical industrial reformer contains an array of catalyst-filled tubes suspended in a huge furnace, supplying the heat for the highly endothermic reforming reactions. These fixed bed reformers are affected by a number of constraints, making them inefficient [2,12].

One of the most serious constraints relates to methane conversion, which is limited by the thermodynamic equilibrium of the reversible reactions. For conventional fixed bed reformers, reaction temperature has to be in the range of 800–900 °C to achieve complete conversion of methane. At this elevated temperature the catalyst undergoes deactivation due to carbon formation, also resulting in blockage of reformer tubes and increased pressure drops [13].

Temperature, pressure and gas composition must be carefully controlled to avoid catalyst deactivation due to coking. Therefore, it will be extremely desirable if newer concepts for production of H<sub>2</sub> by SMR can be developed

which reduce the capital cost compared to the conventional route.

To this aim, the advantages of coupling reaction systems with different forms of in situ separation have been widely reported in the literature. Such hybrid configurations may substantially improve reactant conversion or product selectivity and, for reversible reactions, establish a more favourable reaction equilibrium under conventional reactor operation conditions.

Reaction enhancement, obtained by removing either hydrogen or CO<sub>2</sub>, may enable a lower temperature of operation, which in turn may alleviate the problems associated with catalyst fouling, high process energy requirements and poor energy integration within the plant environment.

The investigation of reactor concepts, which combine at least two process functionalities synergetically within a single unit, has been the subject of considerable attention in industrial and academic research [14–17].

The solutions, which in the different applications involve hydrogen or carbon dioxide, are selective permeation through a membrane or selective permeation through simultaneous reaction of the targeted molecule (e.g. the reaction inhibitor) with a chemical acceptor. The sorption-enhanced reaction process (SERP), involving the addition of a sorbent into the reaction for selectively uptaking one of the products, produces the equilibrium shifting of the reversible reaction according to the Le Chatelier principle [18–21].

Both solutions, below discussed in detail in relation to particular applications, make it possible to run the process at lower temperatures and producing the same methane conversion.

In the case of addition of a CO<sub>2</sub> acceptor to the reactor, carbon dioxide is converted to a solid carbonate as soon as it is formed, shifting the reversible reforming and WGS reaction beyond their conventional thermodynamic limits. Regeneration of the sorbent releases relatively pure CO<sub>2</sub> suitable for sequestration. Internal carbon dioxide removal will also add extra heat to the reforming reaction due to the exothermicity of such reaction.

### 3.1. Membranes

Membranes may act as perm-selective barriers, or as an integral part of the catalytically active surface. Practical issues such as membrane pore blockage, thermal and

mechanical stability, and the dilution caused by the need for sweep (permeate purge) gases, have limited the usefulness of the membrane reactor systems. Nevertheless, the benefits of the membrane systems have been demonstrated through a wide number of experimental reaction studies, examples which include the dehydrogenation of ethane, cyclohexane, ethylbenzene and acetylene and CO<sub>2</sub> production via the SMR and WGS reactions. Particular membranes, for coupled SMR and WGS reaction for H<sub>2</sub> rich syngas production, are described below.

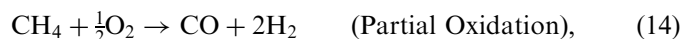
#### 3.1.1. OTM+HTM membrane with porous ceramic substrate and palladium film coating

A lower cost production process of hydrogen is based on reducing the number of processing steps required. *Praxair* has defined the concept that involves integration of syngas generation from natural gas, shift reaction and hydrogen separation into a single membrane-reactor separator [22]. The key elements required to make this possible are an oxygen transport membrane (OTM) and a hydrogen transport membrane (HTM). Both membranes are based on ceramic mixed conducting materials and operate at similar temperatures (800–1000 °C).

The OTM conducts oxygen ions and electrons and has infinite selectivity for oxygen over other gases. Similarly, the HTM conducts only protons and electrons and therefore infinitely selective for hydrogen.

A schematic diagram of the integrated-membrane reactor separator is shown in Fig. 2. The reactor is divided in three compartments by integrating both OTM and HTM into a single unit.

Air at low pressure (~0.17 kPa) is passed to the cathode side of the OTM, while compressed natural gas (1.36–2 kPa) and water/steam are passed to the anode side of OTM. Oxygen is transported across OTM to the anode side, where it reacts with natural gas to form syngas (Eq. (14)). A portion of natural gas also reacts with steam to form syngas (Eq. (15)). Catalyst is incorporated in the reactor to promote reforming reaction.



The syngas side is also exposed to feed side of HTM. Hydrogen is transported through HTM to the permeate

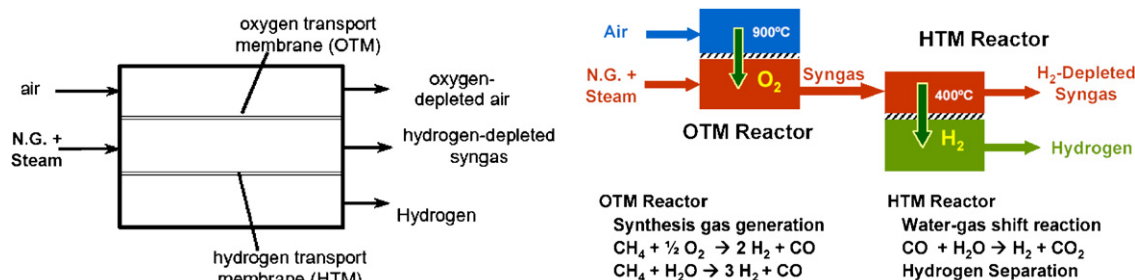


Fig. 2. Integrated-membrane reactor separator.



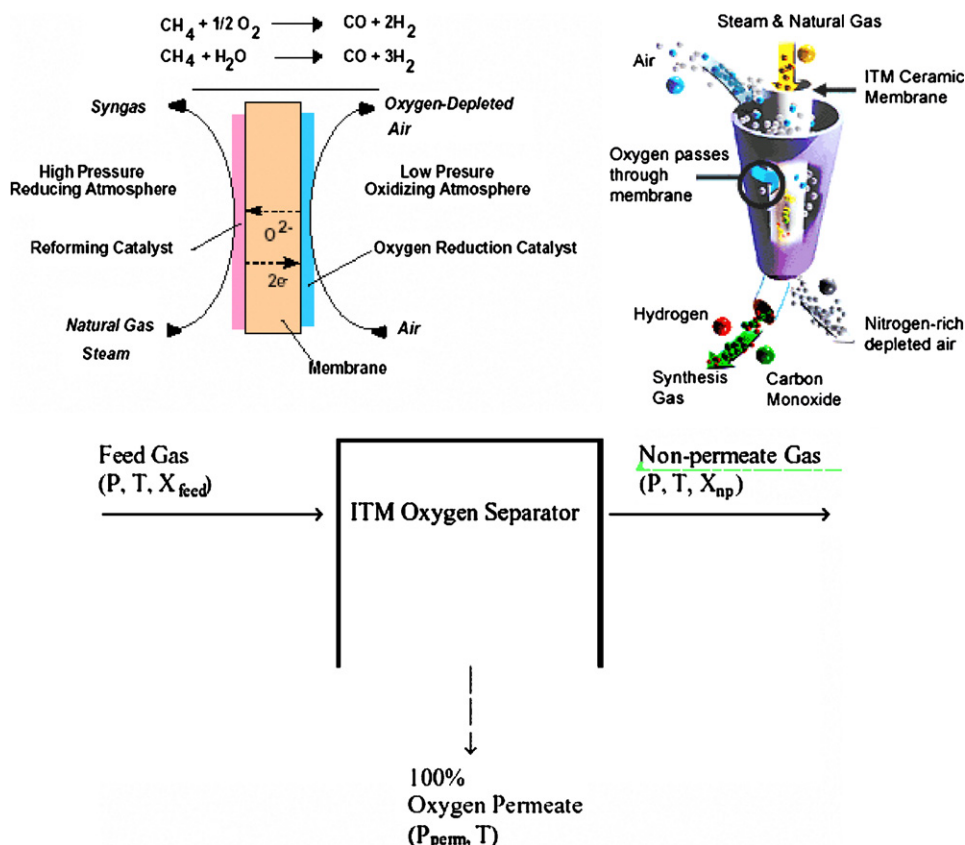
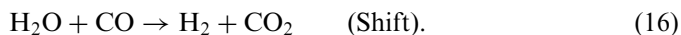


Fig. 3. Process flow diagram of ITM oxygen separator.

side driven by partial pressure difference. Due to removal of hydrogen from the reaction zone, more hydrogen is formed by the shift reaction (Eq. (16)):



As much hydrogen as possible is recovered from the reaction zone by its transport through HTM to the permeate side. When a pinch partial pressure difference between reaction zone and permeate side is reached, no more hydrogen can be recovered.

### 3.1.2. Ion transport membrane (ITM)

The ITMs technology may simplify the hydrogen production from natural gas and its separation by combining these processes into a single step, achieving lower costs and greater efficiencies. ITM systems combine the separation of air to produce oxygen and the subsequent use of that oxygen (in a process called partial oxidation) to generate synthesis gas. The process takes place in a single step (Fig. 3) and it's an air products patent [23].

The technology uses non-porous ceramic membranes fabricated from multi-component metallic oxides that conduct both electrons and oxygen ions at temperatures greater than 700 °C.

During operation, oxygen from a hot air stream is reduced by catalysts at one surface of the membrane to create oxygen ions. The oxygen ions flow through the

membrane under a chemical gradient to the opposite membrane surface where they partially oxidize a pre-reformed hot mixture of steam and natural gas to form synthesis gas, that is a mixture of carbon monoxide and hydrogen. ITM utilizes an oxygen partial pressure differential across the membrane to cause oxygen ions to migrate through the membrane [24]. The ratio of hydrogen to carbon monoxide is partly dependent upon the amount of steam that is used.

The synthesis gas then proceeds to a WGS reactor where additional steam is added to convert the steam and carbon monoxide to more hydrogen and carbon dioxide.

This mixture of hydrogen, carbon dioxide, and trace amounts of carbon monoxide is then separated to produce a hydrogen product stream and a concentrated carbon dioxide stream that can be captured and eventually sequestered.

Membranes can be fabricated as tubes or flat plates that are arranged in modules for efficient contact with the hot compressed air. High-purity oxygen permeate and nitrogen-enriched non permeate products are withdrawn from the modules.

To produce the needed separation between  $\text{H}_2$  stream and a concentrated  $\text{CO}_2$  stream, a second typology of membranes, relating to per-selective barriers systems, can be used. In particular, the following systems are evidenced.

**3.1.2.1. Palladium membrane.** This kind of membrane is made of palladium alloy, which allows only hydrogen to permeate. Installing reforming catalysts and the membrane modules in the same reactor, simultaneous generation and separation of hydrogen is achieved. This not only makes the reactor drastically compact, but also drastically lowers the reaction temperature thanks to the breakage of chemical equilibrium.

The conventional hydrogen production unit, which produces hydrogen from city gas through steam reforming reaction, requires high reaction temperature of 800–900 °C and big hydrogen separation unit, usually based on PSA process, afterwards. However, in the case of membrane made of palladium alloy, the reaction temperature can be lowered to 500–550 °C, which enhances high thermal efficiency, and hydrogen separation unit can be eliminated, which makes the unit as compact as  $\frac{1}{3}$  in volume and  $\frac{1}{2}$  in terms of area of the conventional unit.

The membrane is exposed to severe conditions, still high temperature as 500–550 °C and pressure as about 0.1 Mpa.

However, even under such conditions, palladium alloy membranes have already achieved such high endurance as 1600 h and 30 start-stops and researches still continuing hard efforts to extend their life [25].

**3.1.2.2. Porous inorganic membranes for high temperature hydrogen separation IMTL.** Inorganic membranes with pore sizes less than 1 nm offer many advantages over thin-film palladium membranes and ion-transport membranes for the separation of hydrogen from a mixed-gas stream. In microporous membranes, the flux is directly proportional to the pressure, whereas in palladium membranes it is proportional to the square root of the pressure. Therefore, microporous membranes become the more attractive option for systems that operate at high pressure. Moreover microporous membranes permeance increases dramatically with temperature [26].

Consequently, inorganic membranes have the potential to produce very high fluxes at elevated temperatures and pressures. The membranes can be fabricated from a variety of materials (ceramics and metals) because the separation process is purely physical, not ion transport. Proper material selection can ensure that the membrane will have a long lifetime while maintaining high flux and selectivity.

One further advantage is the relatively low cost of microporous membranes. Because their fabrication does not require the use of exotic materials or precious metals, such as palladium, the cost of producing microporous membranes should be low compared to the one for palladium membranes.

One disadvantage of microporous inorganic membranes is that they are porous. They can never produce 100% pure gas streams as can thin-film-palladium or ion-transport membranes. However, when microporous membranes are coupled with PSA, the combined system can produce 100% hydrogen. In this scenario, PSA would only be required to separate the final 1% of the impurities, and the coupling of the two technologies should result in a very compact and efficient separation system.

### 3.2. Sorption enhanced SMR using CO<sub>2</sub> sorbent

On the other hand, a new field of research for to develop new SMR processes with in situ CO<sub>2</sub> separation, deals with the study of innovative reactors where sorbents are added in order to enhance the reactions. Such process is known as *sorption-enhanced steam methane reforming* (SE-SMR). An innovative plant solution for hydrogen production, developed through the SE-SMR process implementation, is described in [14,15].

The main criteria used to estimate the potentiality of a sorbent for SE-SMR are:

- high reaction rate in the range of temperature 450–650 °C;
- stability of the performances relative to their use in production/regeneration cycles;
- low temperature interval between carbonation and calcination;
- low cost;
- high adsorption ability.

The sorbents mostly used are divided in natural and synthetic ones and they are listed in Table 2.

Calcium carbonate and dolomite are inexpensive, easy to find and characterized by high adsorption ability. Otherwise, the sorbents, constituted mainly by inert, need a greater energy amount for their regeneration. Sintering at high calcination temperatures causes rapid decay in capacity upon multiple re-carbonation. (After 45 cycles, this reduction is less than 20% and about 40% and 60% for huntite, dolomite and calcium carbonate, respectively.) Adsorption reaction is rapid during the early stages, but undergoes an abrupt transition and becomes extremely slow before complete CaO conversion is achieved.

Also listed in Table 2 is the hydrotalcite (HTC), which is an anionic clay consisting of positively charged layers of metal oxide (or metal hydroxide) with inter-layers of anions, such as carbonate. Both adsorption and regeneration temperature is around 400 °C and adsorption/desorption kinetics are relatively fast.

Promoted K<sub>2</sub>CO<sub>3</sub>/HTC was tested by Hufton et al. [32] and it results indeed stable maintaining an equilibrium CO<sub>2</sub> capacity of 0.3–0.45 mmol/g (0.018 g CO<sub>2</sub>/g sorbent) over nearly 6000 cycles. Although high stability upon multi-cycle test, the adsorption capacity is very low, most likely restricting its potential as a sorbent on an industrial scale [20]. Relative to sorbent multi-cycle durability, the research activities are currently focused on the development of new synthetic sorbents with high mechanical stability (some products are indicated in Table 2 together with adsorption ability and regeneration temperature), but their costs of production are still too high and require them to sustain at least 10 000 cycles to compete with natural sorbents [33]. Moreover, the reported rate of reaction for this kind of sorbents is too slow to compete with calcium-based ones.



Table 2  
Stoichiometric capacities and regeneration temperatures for various sorbents

	Sorbent	Stoichiometric adsorption ability (g CO <sub>2</sub> /g sorbent)	Regenerating temperature (°C)	Stoichiometric adsorption ability after 45 cycles
Natural sorbents	Calcium carbonate (CaCO <sub>3</sub> )	0.79	900 <sup>a</sup>	0.316
	Dolomite (CaCO <sub>3</sub> × MgCO <sub>3</sub> )	0.46	900 <sup>a</sup>	0.16
	Huntite (CaCO <sub>3</sub> × 3MgCO <sub>3</sub> )	0.25	900 <sup>a</sup>	0.20
	Hidrotalcite, promoted K <sub>2</sub> CO <sub>3</sub> /hydrotalcite	0.029 <sup>b</sup>	400 <sup>c</sup>	Stable
Synthetic sorbents	Lithium orthosilicate (Li <sub>4</sub> SiO <sub>4</sub> )	0.37	750 <sup>d</sup>	Stable until 100 cycles
	Lithium zirconate (Li <sub>2</sub> ZrO <sub>3</sub> )	0.29	690 <sup>e</sup>	Stable until 100 cycles
	Sodium zirconate (Na <sub>2</sub> ZrO <sub>3</sub> )	0.24	790 <sup>f</sup>	Stable until 100 cycles

<sup>a</sup>Temperature corresponding to CO<sub>2</sub> equilibrium pressure of 1 bar [27].

<sup>b</sup>0.65 mol CO<sub>2</sub>/kg, from Ding and Alpay [28].

<sup>c</sup>Regeneration through pressure swing.

<sup>d</sup>From Essaki and Kato [29].

<sup>e</sup>Experimental data from Yi and Eriksen (regeneration in nitrogen) [30].

<sup>f</sup>Experimental data from Lopez-Ortiz et al. (regeneration in air) [31].

The effectiveness of both SE-SMR and the use of calcium-based CO<sub>2</sub> sorbents have been demonstrated in previous works. In particular, Rostrup-Nielsen [34] reports that the first description of the addition of a CO<sub>2</sub> sorbent to a hydrocarbon-steam-reforming reactor was published in 1868. Williams [35] was issued a patent for a process in which steam and methane react in the presence of a mixture of lime and reforming catalyst to produce hydrogen. A fluidized-bed version of the process was patented by Gorin and Retallick [36]. Brun-Tsekhovoi et al. [37] published limited experimental results and reported potential energy saving of about 20% compared to the conventional process. Recently, Kumar et al. [38] reported on a process known as unmixed combustion (UMC), in which the reforming, shift, and CO<sub>2</sub> removal reactions are carried out simultaneously over a mixture of reforming catalyst and CaO-based CO<sub>2</sub> sorbent.

In related work, Hufton et al. [32] reported on H<sub>2</sub> production through SE-SMR using a K<sub>2</sub>CO<sub>3</sub>-treated HTC sorbent, although the extremely low CO<sub>2</sub> working capacity above discussed. Average purity of H<sub>2</sub> was about 96% while CO and CO<sub>2</sub> contents were less than 50 ppm. The methane conversion to H<sub>2</sub> product reaches 82%. The conversion and product purity are substantially higher than the thermodynamic limits for a catalyst-only reactor operated at these same conditions (28% conversion, 53% H<sub>2</sub>, 13% CO/CO<sub>2</sub>).

In an earlier work, Balasubramanian et al. [39] showed that a gas with a hydrogen content up to 95% (dry basis) could be produced in a single reactor containing reforming catalyst and CaO formed by calcination of high-purity CaCO<sub>3</sub>. The reported methane conversion was 88%.

In the case of using CaO as a sorbent, in addition to reactions of SMR and WGS (Eqs. (1)–(3)), the non catalytic highly exothermic carbonation reaction (Eq. (17)) is included in SE-SMR:

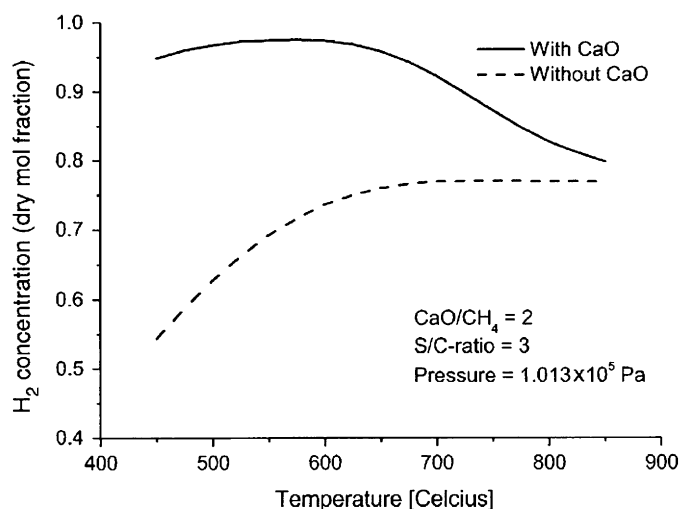
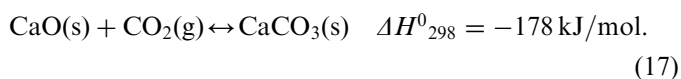


Fig. 4. Hydrogen content at equilibrium as a function of temperature for a pressure of  $1.013 \times 10^5$  Pa, a H<sub>2</sub>O:CH<sub>4</sub> molar ratio of 3 and a CaO:CH<sub>4</sub> molar ratio of 2.

For a calcium oxide sorbent process, the typical operating temperatures are about 500–650 °C.

The advantages of combining steam reforming with in situ CO<sub>2</sub> capture can be seen in thermodynamics. Fig. 4 shows the equilibrium hydrogen concentration as a function of reaction temperature at ambient pressure and with a S/C equal to 3. Sorption enhancement enables both lower reaction temperatures, which may reduce catalyst coking and sintering, and the consequent use of less expensive reactor wall materials. In addition heat released by the exothermic carbonation reaction supplies most of the heat required by the endothermic reforming reactions. However, energy is required to regenerate the sorbent to its oxide form by the energy intensive calcinations reaction (reverse of Eq. (17)). Though many works have related that the energy required for regeneration process is less than 20–25% the supplementary energy required for traditional SMR, thanks to the higher operating temperatures.

Although the SE-SMR can directly produce higher purity  $H_2$  than a conventional catalyst-only reactor, it is not high enough to satisfy high purity customers (99.9 %). Thus, a PSA unit is required to purify the effluent gas. The PSA adds a  $\sim 15\%$  recovery loss to the process, and also requires the feed gas at an high pressure reducing performances of the process. Moreover, the adsorption capacity and chemical stability during carbonation/calcination cycles of the known sorbents must be tested deeply and new improved sorbents should be identified.

### 3.2.1. Kinetic models and parameters for SE-SMR

Adequate design and scale-up of such processes will require information on the kinetics of adsorption and desorption, as well as reaction kinetic models under transient conditions in the presence of a sorbent. In the literature, several works concerning the description of adsorption equilibrium [5] and adsorption kinetics [40], have been reported for high temperature  $CO_2$  adsorption onto HTC-based sorbents. Furthermore, Ding and Alpay [41] proposed a non-isothermal non-isobaric dynamic reactor model to predict the observed species evolution profiles from an adsorptive reactor. Later, Xiu et al. [42] developed a mathematical model taking into account multi-component mass balances, pressure drop and energy balance to describe the SE-SMR cyclic process. The models from Ding and Alpay and Xiu et al. are more realistic for process description; however, due to the highly nonlinear interaction involved in these models, the numerical results are not easy to be interpreted.

The gas–solid  $CO_2$ –CaO reaction proceeds through two rate controlling regimes. At the very initial stage, the reaction occurs rapidly by heterogeneous surface chemical reaction kinetics. Following this initial stage, as compact layer of product  $CaCO_3$  is developed on the outer region of a CaO

particle, the rate of reaction decreases due to the diffusion limitation of reacting species through the layer. The carbonation conversion actually comes to an end when a strong intra-particle diffusion limitation of  $CO_2$  is affected by the compact thick layer of product  $CaCO_3$  developed on the outer region of a CaO particle. The reaction rate dependence on CaO– $CaCO_3$  conversion rate is more effective at low temperatures, while, as shown in Fig. 5, up to  $690^\circ C$  the limited diffusion effect does not influence the process as well. Typical data of the carbonation conversions of CaO on different temperature above  $550^\circ C$  is shown in Fig. 6, where the relationship between CaO concentration and temperature is well represented. The data shown in Fig. 6A relates to the experimental results obtained by Bhatia and Perlmutter [43] while those in Fig. 6B to the experimental study carried out by Gupta and Fan [44]. It has been reported that the reaction does not proceed to the complete conversion of CaO, with ultimate conversions in the range of 70–80% or up to 90% [44].

In order to describe such gas–solid reaction kinetics, various models have been introduced. The most classical ones are the continuous model and the unreacted core model [45].

Because the *continuous model* assumes that the diffusion of gaseous reactant into a particle is rapid enough compared to chemical reaction, it is not good for representing the CaO carbonation reaction in diffusion control regime. *Unreacted core model*, known as shrinking core model, assumes that the reaction zone is restricted to a thin front advancing from the outer surface into the particle, which is represented by

$$\frac{t}{\tau} = 1 - (1 - X)^{1/3}, \quad (18)$$

$$\frac{t}{\tau} = 1 - 3(1 - X)^{2/3} + 2(1 - X), \quad (19)$$

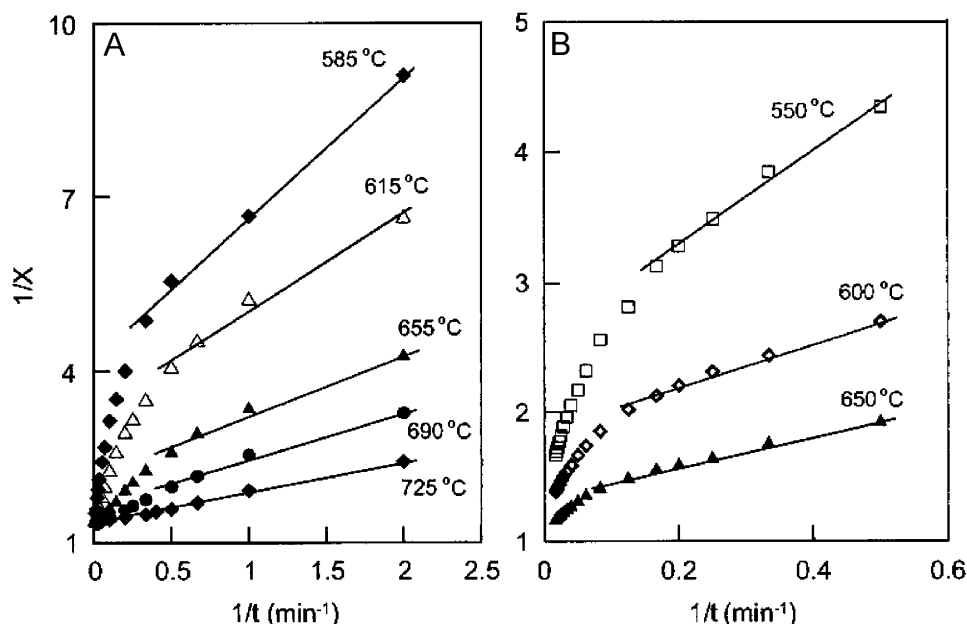


Fig. 5. Plot of  $1/X$  vs  $1/t$  for the conversion data of: (A) Bathia and Perlmutter [43] and (B) Gupta and Fan [44].

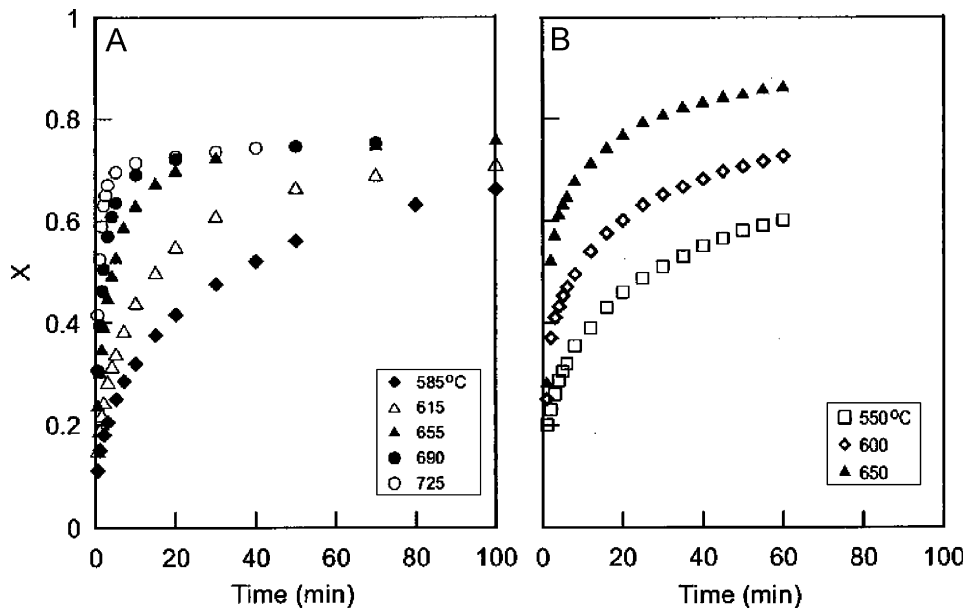


Fig. 6. Carbonation of CaO adopted from the paper of: (A) Bathia and Perlmutter and (B) that of Gupta and Fan.

where

- $t$  is the time;
- $X$  the fractional conversion of CaO to  $\text{CaCO}_3$ ;
- $\tau$  is the time required to completely convert an unreacted particle into product.

While Eq. (18) is for chemical reaction control regime, Eq. (19) is for diffusion control regime. This model could be applied for the CaO-carbonation reaction kinetics.

However, as the model predicts the CaO complete conversion ( $X = 1$  at  $t = \tau$ ), it is not good to properly describe the actual kinetic behaviour in the diffusion control regime of CaO-carbonation. It is also inconvenient to get the conversion using this model because the conversion  $X$  is implicitly given as a function of time.

Bhatia and Perlmutter [43] developed the random pore model, which is represented by Eqs. (20) and (21), to correlate reaction behaviour with the internal pore structure:

$$\frac{1}{\Psi} [\sqrt{1 - \Psi \ln(1 - X)} - 1] = k' t \quad \text{chemical reaction control regime,} \quad (20)$$

$$\frac{1}{\Psi} [\sqrt{1 - \Psi \ln(1 - X)} - 1] = k'' t \quad \text{diffusion control regime,} \quad (21)$$

where

- $\Psi$  is a structural parameter depending on the surface area, porosity, and the initial total length of pore system per unit volume;
- $k'$ ,  $k''$  are rate constants.

Eq. (20) relates to the chemical reaction control regime, and Eq. (21) to the diffusion control regime; in [43] Bathia and Perlmutter have employed Eq. (21) to obtain kinetic parameters.

Bhatia and Perlmutter also reported in [46] that the rate of CaO carbonation was independent of  $\text{CO}_2$  partial pressure, except for a slight effect at a very early stage of the carbonation. Dedman and Owen [47] also reported that the reaction was zero order with respect to  $\text{CO}_2$  pressure.

With respect to the reaction rate being independent of the bulk concentration of the  $\text{CO}_2$ , Lee [48] suggested an apparent kinetic expression for the carbonation of CaO as follows:

$$\frac{dX}{dt} = k_c \left(1 - \frac{X}{X_U}\right)^n \quad n = 1, 2, \quad (22)$$

where:

- $k_c$  is an apparent kinetic rate constant which is dependent on temperature;
- $X_U$  is the ultimate conversion of CaO, at which no more significant conversion is attained at a given temperature and the rate of carbonation becomes negligible in practice.

Moreover, testing the model on the experimental CaO conversion data, gathered by Bathia and Perlmutter [43] (Fig. 6A) and Gupta and Fan [44] (Fig. 6B), Lee have demonstrated by means of list-square regression analysis that the case of exponent  $n = 2$  produces a better approximation.

In this case, integration of Eq. (22) leads to

$$X = \frac{X_U t}{X_U/k + t}. \quad (23)$$

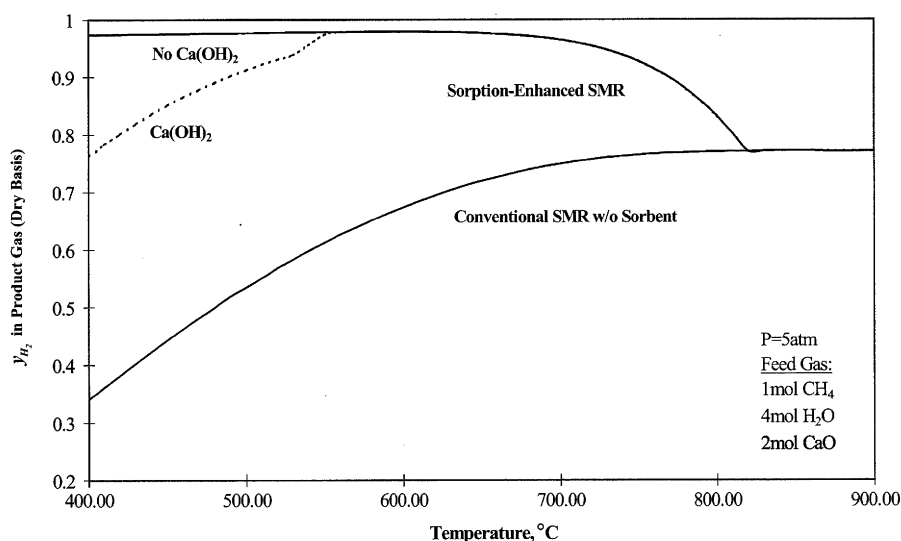


Fig. 7. Equilibrium  $H_2$  molar fraction (dry basis) in the product gas with and without the CaO-based acceptor as a function of temperature at fixed pressure and  $S/C$ .

If a constant  $b$  is introduced as the time taken to attain half the ultimate conversion ( $X = X_U/2$  per  $t = b$ ), the ultimate conversion, resulting by applying Eq. (23) is expressed by

$$X_U = k_c b. \quad (24)$$

Accordingly, the final equation for conversion as a function of time is given by

$$X = \frac{k_c b t}{b + t}, \quad (25)$$

and then, the molar rate of  $CO_2$  removed by the CaO-carbonation is described by

$$r_{CO_2} = \frac{1}{M_{CaO}} \left( \frac{dX}{dt} \right), \quad (26)$$

where  $r_{CO_2}$  is the molar rate of  $CO_2$  removed per unit mass of CaO and  $M_{CaO}$  is the molecular weight of CaO, being  $r_{CO_2}$  independent from gas phase concentration of  $CO_2$ .

### 3.2.2. Temperature and pressure influence on SE-SMR and performances comparison with SMR

Equilibrium  $H_2$  molar fraction (dry basis) in the product gas with and without the CaO-based acceptor is compared in Fig. 7 as a function of temperature at fixed pressure (5 bar) and Steam to Carbon ratio ( $S/C = 4$ ).

At a fixed pressure in the conventional process (without acceptor) the  $H_2$  concentration increases at the temperature increment and reaches a maximum of 0.77 at 800 °C, while in the SE-SMR the maximum is reached at 580 °C with a value of  $H_2$  molar fraction of 0.98. Relative to the SE-SMR process, when the temperature is less than 575 °C the equilibrium  $H_2$  content curve shows two branches: the lower one allows for the formation of both  $CaCO_3$  and  $Ca(OH)_2$ , while  $Ca(OH)_2$  is not formed in the upper branch.

$H_2$  molar fraction is evidently higher for SE-SMR than for traditional SMR and, only for temperatures up to

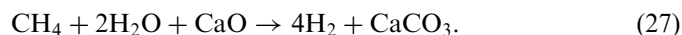
820 °C (corresponding to operational condition highly critical for the  $CO_2$ –CaO reaction), the molar fraction is the same for the two cases.

The influence of temperature on equilibrium  $H_2$  molar fraction is also shown in Fig. 8.

The SMR reactions are not favourite when temperature decreases (until it reaches 400 °C) and consequently both the methane conversion rate and  $CO_2$  formation decrease; this condition, as well as the  $Ca(OH)_2$  formation (typically favoured at low temperature), makes the benefits of  $CO_2$  adsorption (high purity hydrogen in a single step) negligible.

Moreover, for high temperature, although the high  $CO_2$  production rate in the SMR reaction,  $CO_2$  has a low affinity to react because of the exothermicity of the SMR reaction. Infact, up to 800 °C the SE-SMR and the traditional SMR are the same in terms of composition of the product gas. The maximum  $H_2$  molar fraction (dry basis) in the product gas, at a pressure of 5 atm, is reached at 650 °C.

From the thermodynamic equilibrium point of view, lower pressure promotes the production of  $H_2$ . This is shown by the overall reaction expressed by Eq. (27), which entails an increase in the total number of gas phase moles.



The production of  $Ca(OH)_2$  has been experimentally analysed by Hildenbrand et al. [49], during carbonation reaction using natural dolomite ( $Ca_{0.5}Mg_{0.5}CO_3$ ) as internal carbon dioxide sorbent in a fluidized bed reactor.

In the experiments a relatively pure dolomite was used, containing 0.05 wt% Al, and <10 ppm of other elements such as Cu, Ni, Zn, V, Cr and Co, and <1 ppm of heavy metals such as Pb, Cd and Hg. The dolomite was crushed and sieved before use. The 70–170 mesh fraction (90–200  $\mu m$ ) was then calcined at 900 °C in air before

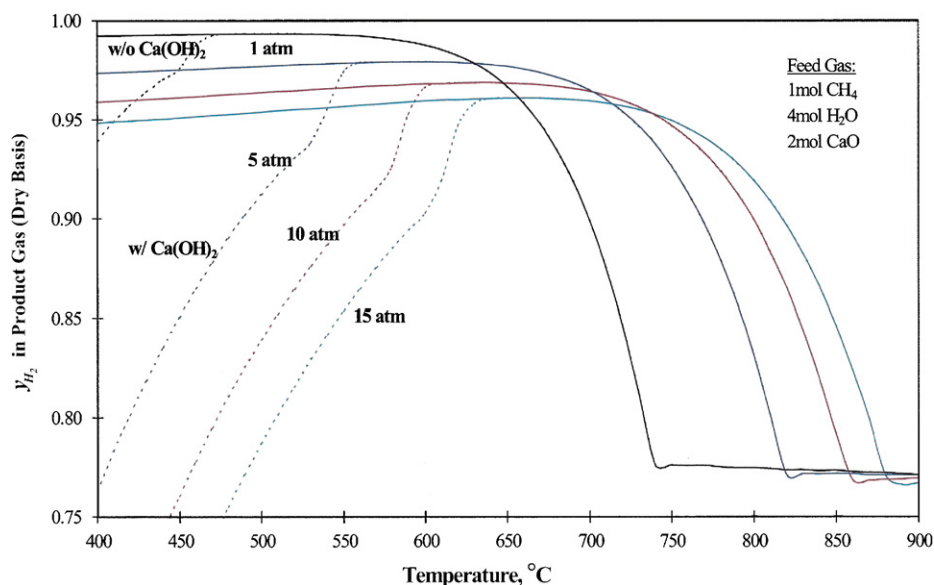


Fig. 8. Equilibrium  $H_2$  molar fraction (dry basis) in the product gas as a function of temperature at several pressures.

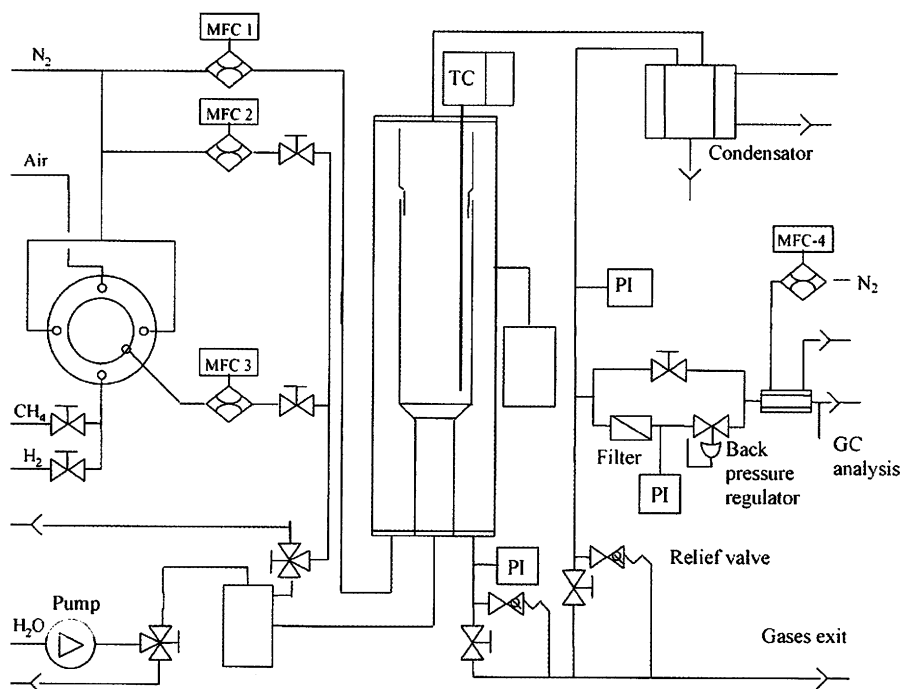


Fig. 9. Schematic drawing of the high pressure fluidized bed reactor rig used.

use. A high nickel loading  $NiO/NiAl_2O_4$  catalyst was prepared in a similar manner as described by Ishida et al [50]. Steam reforming was carried out in a quartz fluidized bed reactor with inner diameter of approximately 25 mm. A schematic drawing of the reactor rig is shown in Fig. 9. The quartz reactor is mounted inside a stainless steel tube so it is possible to run the reactor at pressures up to at least 10 bar. All experiments were carried out by feeding a constant flow of nitrogen into the void between the quartz reactor and the stainless steel tube to maintain the same pressure on each side of the quartz insert. The tests were carried out at 5 bar and 580 °C.

Typically, 8 g catalyst was used together with 12 g dolomite sorbent or alumina. In all the experiments the total flow through the catalyst/sorbent bed was 300 ml(STP)/min which was found to be well above the minimum fluidization condition in the bubbling regime giving minimal attrition.

The experimental results indicate that calcined dolomite has a certain affinity towards water and that water does not solely react with methane according to the reforming reaction, but it also reacts with the sorbent:





Then, reaction 28 will decrease the actual  $\text{H}_2\text{O}/\text{CH}_4$  ratio in the reactor thus lowering the methane conversion and hydrogen yield. After a certain time (induction time) the formation of  $\text{Ca}(\text{OH})_2$  has reached equilibrium leading to a higher  $\text{H}_2\text{O}/\text{CH}_4$  ratio and thus higher conversion of methane. The stability of  $\text{Ca}(\text{OH})_2$  decreases with increased temperature [51], so the induction period is expected to be shorter than the higher the temperature of the SE-SMR reaction. Indeed, Harrison et al. [52] show negligible induction period in their study using dolomite at 650 °C.

Another concern in the SMR process for the production of  $\text{H}_2$ , is the content of CO in the dry product gas, especially for some applications such as fuel cells, that poison the catalyst. The equilibrium concentration of CO content is affected by both pressure and temperature. At a fixed pressure, equilibrium concentration of CO increased with increasing temperature. Infact, higher temperature promotes the endothermic reforming reaction while it inhibits the exothermic WGS reaction and carbonation reaction.

Relative to the CO content in the product gas as a function of pressure, the following aspects can be evidenced:

- the carbonation reaction involves elimination of gas phase moles, its then favoured by high pressure;
- the SMR reaction yields an increase in the total moles in the gas phase and therefore higher pressure limits the formation of CO, which is in the product side of this reaction;
- the WGS reaction is not affected by pressure because there is no change in the total moles in the gas phase.

### 3.2.3. Experimental activities about the characterization of some SE-SMR performances

Ding and Alpay [41] have demonstrated that the steady-state kinetic model of Xu and Froment [11] for SMR has been shown to be applicable to transient reactor operation, both in the presence or absence of a sorbent. The reactor consisted of a stainless-steel tubular column of internal diameter 12.4 mm and length 220 mm, packed with a mixture of catalyst and sorbent particles. Operating conditions were fixed equal to 455 °C and 4.45 bar;  $S/C$  was 3. A commercial Ni-based catalyst (United Catalyst Inc.) containing 25–35% Ni, 2–35% NiO, 5–15% MgO and 1–25% sodium silicate, was used in this work. The  $\text{CO}_2$  sorbent consisted of industrially supplied potassium promoted HTC. For the reaction studies in the absence of the sorbent, approximately 7.2 g of catalyst was admixed with dense silicon carbide particles (about 1:3 mass ratio), and packed into the reactor. For the sorption-enhanced reaction studies, approximately 7.2 g of catalyst was admixed with 14.8 g of  $\text{CO}_2$  adsorbent.

Results obtained from a mathematical model also developed by the authors to describe both the SMR and SE-SMR processes are agreement with experiments.

Therefore, the rate expressions proposed by Xu and Froment are suitable for both the transient and steady-state periods of operation, even in the presence of adsorbent. This suggests that the microkinetic dynamics of carbonation reaction are relatively fast, that the physically admixed nature of catalyst and adsorbent precludes any local effect of adsorption on reaction intermediates and hence on molecular kinetic steps.

Balasubramaniam et al. [39] have conducted experimental studies using a laboratory-scale fixed bed reactor, containing a mixture of commercial reforming catalyst and CaO obtained by calcining high-purity (99.97%)  $\text{CaCO}_3$ , for temperatures varying from 450 to 750 °C. Calcination was performed using a quartz boat in a tube furnace at 750 °C and 1 atm under flowing nitrogen for 4 h. A range of particle sizes from 45 to 210  $\mu\text{m}$  was used in the tests.

The reforming catalyst consisted of NiO (22%) supported on  $\text{Al}_2\text{O}_3$ . The catalyst particles were crushed and sieved with 150  $\mu\text{m}$  particles used in all runs. All reaction tests were conducted at 15 atm and with a  $S/C$  equal to 4. The response from a typical reaction test is shown in Fig. 10, where the mol percents of  $\text{H}_2$ ,  $\text{CH}_4$ , CO, and  $\text{CO}_2$  in the product gas are plotted versus time.

The trends can be divided in four regions:

- an unsteady-state start up period, essentially due to the time needed for reduction of NiO to Ni and then for catalyst activation;
- a first period, called prebreakthrough, throughout all the reactions run at their maximum efficiency and the molar fractions are near to the equilibrium one;
- an interval, breakthrough, during which the adsorption reaction efficiency starts decreasing;
- at last, a period called postbreakthrough, corresponding to about zero adsorption reaction rate and where only the reforming reactions occur.

The authors reported that the fractional conversion of CaO to  $\text{CaCO}_3$  was 0.52 at the end of the prebreakthrough period and 0.71 at the beginning of postbreakthrough. Fractional conversion then increases slowly to 0.73 when the test was completed. Balasubramaniam et al. also reported that, approximately 88% conversion of  $\text{CH}_4$  is thermodynamically feasible and the product gas contains about 95%  $\text{H}_2$ .

Finally, Ortiz and Harrison [53] reported experimental results tests from a laboratory-scale fixed-bed reactor using inexpensive dolomite as the sorbent precursor: the multi-cycle durability of the catalyst–sorbent mixture was studied as a function of regenerating temperature and gas composition. A schematic diagram of the laboratory scale fixed-bed reactor is shown in Fig. 11.

Multicycle tests showed no significant decrease in the maximum  $\text{H}_2$  concentration or increase in the breakthrough time (a measure of global reaction rate) except for regeneration carried out in  $\text{N}_2$  at 950 °C. However, decreases in the fractional sorbent conversion at the

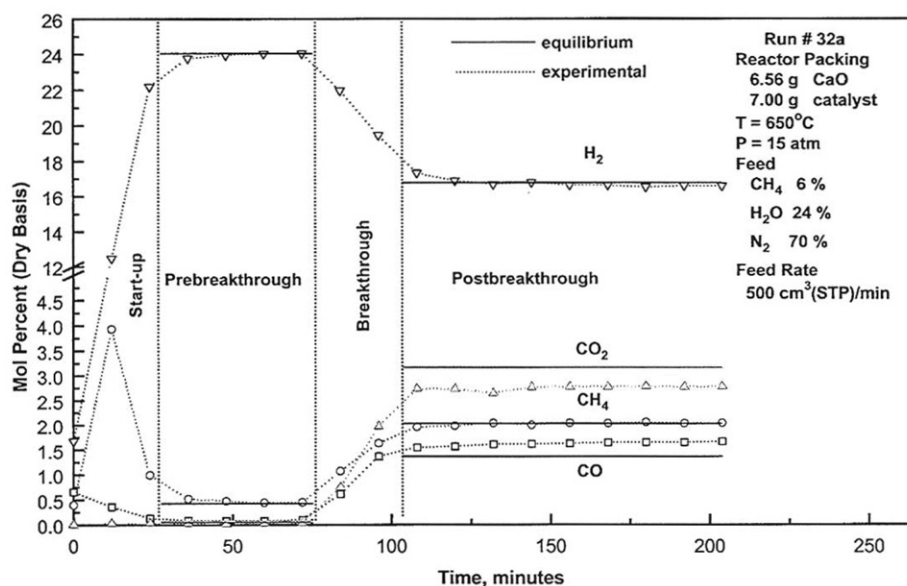


Fig. 10. Typical reactor response curve from [39].

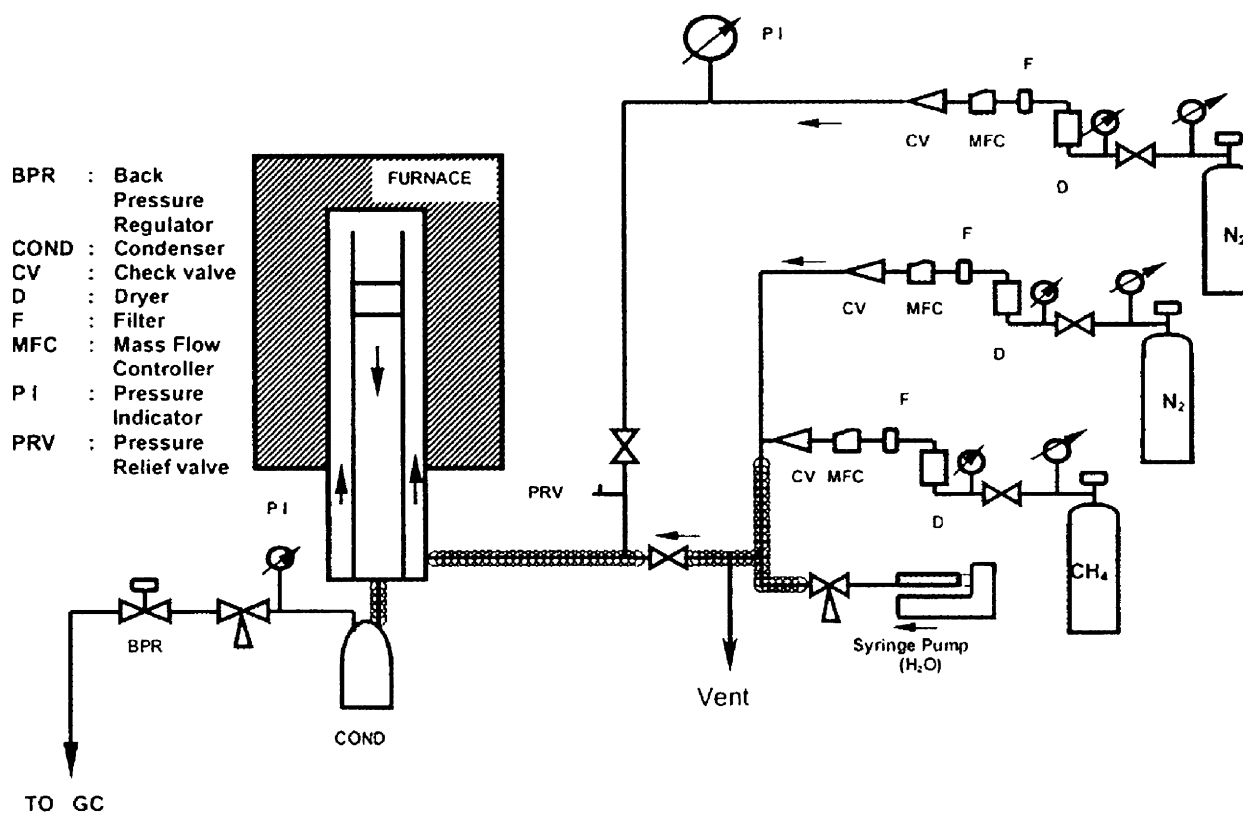


Fig. 11. Schematic of the laboratory-scale fixed bed reactor system from [53].

beginning of breakthrough were detected in all multicycle tests: some loss of activity (see Section 3.2) is inevitable because of the severe conditions required for the regeneration process.

Johnsen et al. [54] conducted a similar experimental study in a fluidized bed and demonstrated that hydrogen concentration remained at 98–99 vol% after four cycles.

#### 4. Conclusions

The dominant industrial process used to produce hydrogen is the steam methane reforming (SMR) process. Although the SMR process has been used for many years, there are numerous areas for improvement. In particular, the investigation of reactor concepts, which combine at

least two process functionalities synergetically within a single unit, has been the object of considerable attention in industrial and academic research.

From the analysis of the technical literature, solutions to enhance the SMR process arise. The significant points relate to the hydrogen removal by selective permeation through a membrane, or selective permeation through simultaneous reaction of the targeted molecule (e.g. the reaction inhibitor) with a chemical acceptor. In particular, significant improvements result in the case of addition of a CO<sub>2</sub> acceptor to the reactor. In such case, in fact, carbon dioxide is converted to a solid carbonate as soon as it is formed, shifting the reversible reforming and WGS reaction beyond their conventional thermodynamic limits, while the regeneration of the sorbent releases a mixture of relatively pure CO<sub>2</sub> and inert gas.

The activity carried out by the authors, as described in [14,15], refers to the latter research path, concerning the development of an innovative hydrogen production system based on a new carbonation reactor. For this reason, in the review process the attention was focused mainly on the SE-SMR to verify the process effectiveness and the critical aspects to overcome in its implementation.

The interesting results found in the literature have encouraged the authors' research and provided a technical database necessary to the development of the carbonation reactor model. In particular, the analysis of kinetic models and experimental data found in the literature and discussed in this paper are the basis for the development of a thermo-fluido-dynamic reactor model that will be used like aid to the carbonation reactor design.

## References

- [1] Twigg MW. Catalyst handbook. England: Wolfe Publishing Ltd; 1989.
- [2] Adris AM, Pruden BB, Lim CJ, Grace JR. On the reported attempts to radically improve the performance of the steam methane reforming reactor. *Can J Chem Eng* 1996;74:177.
- [3] Leiby SM. Options for refinery hydrogen PEP report no. 212, process economic program. Menlo Park, CA: SRI International; 1984.
- [4] Kirk-Othmer X. Concise encyclopedia of chemical technology, vol. 12, 4th ed. New York: Wiley; 1999. p. 950.
- [5] Hufton JR, Mayorga S, Sircar S. Sorption enhanced process for hydrogen production. *AIChE J* 1999;45:248–56.
- [6] Voss C. Applications of pressure swing adsorption technology. *Adsorption* 2005;11:527–9.
- [7] Warmuzinski K, Tanczyk M. Multicomponent pressure swing adsorption. Part I: modelling of a large scale PSA installations. *Chem Eng Process* 1997;36:89–99.
- [8] Hou K, Hughes R. The kinetics of methane steam reforming over a Ni/a-Al<sub>2</sub>O catalyst. *Chem Eng J* 2001;82:311–28.
- [9] Castro Luna AE, Becerra AM. Kinetics of methane steam reforming on a Ni on alumina–titania catalyst. *React Kinet Catal Lett* 1997;61:369–74.
- [10] Hoang DL, Chan SH, Ding OL. Kinetic and modelling study of methane steam reforming over sulfide nickel catalyst on a gamma alumina support. *Chem Eng J* 2005;112:1–11.
- [11] Xu JG, Froment GF. Methane-steam reforming, methanation and water gas shift—I: intrinsic kinetics. *AIChE J* 1989;35:88–96.
- [12] Chen Z, Yan Y, Elnashaie SSEH. Novel circulating fast fluidized-bed membrane reformer for efficient production of hydrogen from steam reforming of methane. *Chem Eng Sci* 2003;58:4335–49.
- [13] Trimm DL. Coke formation and minimization during steam reforming reactions. *Catal Today* 1997;37(3):233–8.
- [14] Barelli L, Bidini G, Corradetti A, Desideri U. Study of the carbonation–calcination reaction applied to the hydrogen production from syngas. *Energy* 2007;32:697–710 [Elsevier, articolo n. EGY-1789].
- [15] Barelli L, Bidini G, Corradetti A, Desideri U. Production of hydrogen through the carbonation–calcination reaction applied to CH<sub>4</sub>/CO<sub>2</sub> mixtures. *Energy* 2007;32:834–43 [Elsevier, articolo n. EGY-1809].
- [16] Agar DW, Ruppel W. *Chem Eng Technol* 1988;60:731–41.
- [17] Krishna R. Reactive separations: more ways to skin a cat. *Chem Eng Sci* 2002;57:1491–504.
- [18] Xiu GH, Li P, Rodrigues AE. Sorption enhanced reaction process with reactive regeneration. *Chem Eng Sci* 2002;57:3893–908.
- [19] Xiu GH, Li P, Rodrigues AE. New generalized strategy for improving sorption-enhanced reaction process. *Chem Eng Sci* 2003; 58:3425–37.
- [20] Reijers HTJ, Valster-Schiermeier SEA, Cobden PD, Van der Brink RW. Hydrotalcite as CO<sub>2</sub> sorbent for sorption-enhanced steam reforming of methane. *Ind Eng Chem Res* 2006;45:2522–30.
- [21] Yong Z, Mata V, Rodrigues AE. Adsorption of carbon dioxide onto hydrotalcite-like compounds (HTLcs) at high temperatures. *Ind Eng Chem Res* 2001;40:204–9.
- [22] Shah MM, Drnevich RF, Balachandran U. Integrated ceramic membrane system for hydrogen production. In: Proceedings of the 2000 hydrogen program review NREL/CP-570-28890.
- [23] Air products and chemicals “Ion transport membrane module and vessel system” USP 10/635,695.
- [24] Wright JD, Copeland RJ. Report no. TDA-GRI-90/0303, Gas Research Institute, September 1990.
- [25] Roy S, Cox BG, Adris AM, Pruden BB. Economics and simulation of fluidized bed membrane reforming. *Int J Hydrogen Energy* 1998; 23(9):745.
- [26] Bischoff BL, Judkins RR. Development of inorganic membranes for Hydrogen separation. Oak Ridge National Laboratory.
- [27] Baker EH. The calcium oxide–carbon dioxide system in the pressure range 1–300 atmospheres. *J Chem Soc* 1962;70:464–70.
- [28] Ding Y, Alpay E. Equilibria and kinetics of CO<sub>2</sub> adsorption on hydrotalcite adsorbent. *Chem Eng Sci* 2000;55:3461–74.
- [29] Essaki K, Kato M. Influence of temperature and CO<sub>2</sub> concentration on the CO<sub>2</sub> absorption properties of lithium silicate pellets. *J Mater Sci* 2005;40:5017–9.
- [30] Yi KB, Eriksen D. Low temperature liquid state synthesis of lithium zirconate and its characteristics as a CO<sub>2</sub> sorbent. *Sep Sci Technol* 2006;41:283–96.
- [31] Lopez-Ortiz A, Perez Riviera NG, Reyes Rojas A, Lardizabal Gutierrez D. Novel carbon dioxide solid acceptors using sodium containing oxides. *Sep Sci Technol* 2004;39:3559–72.
- [32] Hufton J, Waldron W, Weigel S, Rao M, Nataraj S, Sircar S. Sorption enhanced reaction process (SERP) for the production of hydrogen. Allentown, PA 18195: Air Products and Chemicals, Inc.
- [33] Abanades JC, Rubin ES, Anthony EJ. Sorbent cost and performance in CO<sub>2</sub> capture systems. *Ind Eng Chem Res* 2004;43:3462–6.
- [34] Rostrup-Nielsen J. In: Anderson JR, Boudart M, editors. Catalytic steam reforming catalysis science and technology. Berlin: Springer; 1984.
- [35] Williams R. Hydrogen production. US patent 1,938,202, 1933.
- [36] Gorin E, Retallick WB. Method for the production of hydrogen. US patent 3,108,857, 1963.
- [37] Brun-Tsekhovoi AR, Zadorin AN, Katsobashvili YR, Kourdyumov SS. The process of catalytic steam-reforming of hydrocarbons in the presence of a carbon dioxide acceptor. In: Veziroglu TN, Protsenko AN, editors. Hydrogen energy progress VII, proceedings of the seventh world hydrogen energy conference, Moscow, Russia, September 25–29, vol. 2. New York: Pergamon Press; 1988. p. 885.

- [38] Kumar R, Cole J, Lyon R. Unmixed reforming: an advanced steam reforming Process presented at the fuel cell reformer conference, South Coast Air Quality District, Diamond Bar, CA, 1999.
- [39] Balasubramanian B, Lopez Ortiz A, Kaytakoglu S, Harrison DP. Hydrogen from methane in a single-step process. *Chem Eng Sci* 1999;54:3543.
- [40] Soares JL, Moreira R, José HJ, Grande C, Rodrigues AE. *Sep Sci Technol* 2004;39:1989–2010.
- [41] Ding Y, Alpay E. Adsorption-enhanced steam methane reforming. *Chem Eng Sci* 2000;55:3929–40.
- [42] Xiu GH, Soares JL, Li P, Rodrigues AE. *AIChE J* 2002;48:2817–32.
- [43] Bhatia SK, Perlmutter DD. *AIChE J* 1983;29(1):79.
- [44] Gupta H, Fan LS. *Ind Eng Chem Res* 2002;41:4035.
- [45] Kunii D, Levenspiel O. *Fluidization engineering*. New York: Wiley; 1969. p. 480–9.
- [46] Bhatia SK, Perlmutter DD. Effect of the product layer on the kinetics of the  $\text{CO}_2$ –lime reaction. *AIChE J* 1983;29:79–86.
- [47] Dedman AJ, Owen AJ. Calcium cyanamide synthesis part 4—the reaction  $\text{CaO} + \text{CO}_2 = \text{CaCO}_3$ . *Trans Faraday Soc* 1962;58:2027–35.
- [48] Lee DK. An apparent kinetic model for the carbonation of calcium oxide by carbon dioxide. *Chem Eng J* 2004;100:71–7.
- [49] Hildenbrand N, Readman J, Dahl IM, Blom R. Sorbent enhanced steam reforming (SESR) of methane using dolomite as internal carbon dioxide absorbent: limitations due to  $\text{Ca(OH)}_2$  formation. *Appl Catal A Gen* 2006;303:131–7.
- [50] Ishida M, Yamamoto M, Ohba T. Experimental results of chemical-looping combustion with  $\text{NiO/NiAl}_2\text{O}_4$  particle circulation at 1200 °C. *Energy Convers Manage* 2002;43:1469.
- [51] Lin S, Harada M, Suzuki Y, Hatano H. Hydrogen production from coal by separating carbon dioxide during gasification. *Fuel* 2002;81:2079.
- [52] *Chem Eng Commun* 1996;146:149; *Phys Chem Chem Phys* 2005;7:1214.
- [53] Ortiz AL, Harrison DP. Hydrogen production using sorption-enhanced reaction. *Ind Eng Chem Res* 2001;40:5102–9.
- [54] Johnsen K, Ryu HJ, Grace JR, Lim CJ. Sorption-enhanced steam reforming of methane in a fluidized bed reactor with dolomite as  $\text{CO}_2$ -acceptor. *Chem Eng Sci* 2006;61:1195–202.